VARIATIONS IN PLASMA WAVE INTENSITY WITH DISTANCE ALONG THE ELECTRON FORESHOCK BOUNDARY AT VENUS

G. K. Crawford, R. J. Strangeway and C. T. Russell

Institute of Geophysics and Planetary Physics, University of California at Los Angeles, Los Angeles, CA 90024-1567, U. S. A.

ABSTRACT

Plasma waves are observed in the solar wind upstream of the Venus bow shock by the Pioneer Venus Orbiter. These wave signatures occur during periods when the interplanetary magnetic field through the spacecraft position intersects the bow shock, thereby placing the spacecraft in the foreshock region. Wave intensity is analyzed as a function of distance along the electron foreshock boundary. We find that the peak wave intensity may increase along the foreshock boundary from the tangent point to a maximum value at several Venus radii, then decrease in intensity with subsequent increase in distance. These observations could be associated with the instability process: the instability of the distribution function increasing with distance from the tangent point to saturation at the peak. Thermalization of the beam for distances beyond this point could reduce the distribution function instability resulting in weaker wave signatures.

INTRODUCTION

The Pioneer Venus Orbiter (PVO) spacecraft has been in orbit around Venus and collecting data for over 10 years. In the solar wind upstream of the Venus bow shock, this spacecraft has observed plasma waves similar in nature to those upstream of Earth's bow shock. The wave observations coincide to periods when the Interplanetary Magnetic Field (IMF), through the spacecraft position, intersects the bow shock thereby placing the spacecraft in the foreshock region. This magnetic connectivity provides a source for backstreaming charged particles which have been both energized and reflected at the bow shock. The counterstreaming beams of charged particles can interact with charged particles in the solar wind via streaming plasma instabilities to generate the observed waves. Various regions within the foreshock are sampled as temporal changes in the IMF orientation cause corresponding changes in the spacecraft location within the foreshock region.

Study of the Venus foreshock offers a distinct advantage over similar studies at Earth. Pressure balance required to standoff the solar wind flow is achieved at Earth via magnetic pressure in the magnetosphere whereas Venus uses thermal pressure in the ionosphere. Such an obstacle is not subject to rapid large scale fluctuations in size and shape as observed for the Earth. It has been shown /1/ that the Venus bow shock, though changing in size with changing solar wind conditions, maintains a relatively constant shape (eccentricity of 0.66) over an entire solar cycle. Also, the changes in obstacle size are on a much smaller scale than those at Earth. Thus, due to the stability of the ionospheric obstacle, we can model the Venus bow shock and predict the foreshock boundary with greater accuracy than is possible at Earth.

Many studies of the foreshock region have been carried out at Earth /2-5/. It is our intent to apply the insight into foreshock plasma processes and their accompanying wave signatures, gained from these past studies at Earth, towards an understanding of the foreshocks of unmagnetized obstacles. Progress has been made in this regard by a previous study /6/. This study found that the electron foreshock boundary was clearly evident in the wave data and that wave intensity, when parameterized by foreshock penetration depth (see geometry in Figure 1), peaked sharply at the foreshock boundary, then quickly dropped in intensity with greater penetration into the foreshock. The current study considers a different aspect of the foreshock plasma wave behavior than that addressed in /6/: variation in wave intensity with distance along the electron foreshock boundary.

EXPERIMENTAL

The plasma wave observations were made with the PVO Orbiter Electric Field Detector (OEFD) /7/. Measurements are made in 4 continuously active channels with center frequencies of 30 kHz, 5.4 kHz, 730 Hz, and 100 Hz. However, only the 30 kHz channel detects waves at the electron plasma frequency which reflect our observations in the electron foreshock. (Note: The plasma frequency in the solar wind at 0.72 AU under normal solar wind conditions is ~ 30 kHz corresponding to a density of 10 cm^{-3}).

Since the position of the spacecraft with respect to the bow shock and the electron foreshock boundary varies with magnetic field orientation, we use the magnetic field measured by the orbiter magnetometer (OMAG, /8/) to specify our coordinate system. These local magnetic field measurements are then applied to determine when the field line through the spacecraft position intersects a model bow shock thereby establishing connectivity. The shock model is taken from /9/ and is a conic of revolution with focus at the center of the planet. The shock size is adjusted using observed shock crossings in the data. In the velocity aberrated coordinate system the shock is considered to be cylindrically symmetric about the aberrated **x** (Venus-Sun) axis. The effect of slight asymmetries in the shock about this axis due to ion-pickup and other plasma processes is assumed to be negligible.

Besides determining if the spacecraft is magnetically connected to the shock, we define the electron foreshock boundary and the distance along this boundary from the tangent point. To the resolution of OEFD data, observations of the electron foreshock boundary cannot be separated from the shock tangent line, thus the two terms are used synonymously in this study. Our geometry is shown in Figure 1. Different regions of the foreshock are sampled as variations in the IMF orientation cause both the location of the spacecraft relative to the foreshock boundary and the point of intersection of the field line on the shock surface to change.

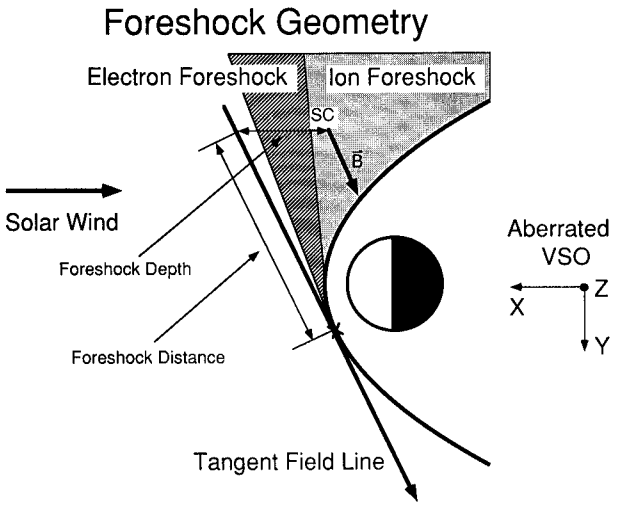

Fig. 1. Foreshock geometry used in this study. The coordinate system is defined by first rotating into the velocity aberrated frame and then ordering the coordinate system by the IMF. In such a coordinate system the shock is cylindrically symmetric about the x axis and all variation in the IMF is in the x-y plane. Distance is measured along the tangent line from the tangent point.

OBSERVATIONS AND DISCUSSION

Solar wind electrons which are reflected and energized at the shock will propagate back upstream, as electron beams, along the IMF lines connected to the shock. From our previous results /6/, we expect a correlation of wave intensity with depth due to convection of these beams by the solar wind. In that study, random orbits were examined and selected for analysis if they showed at least some 30 kHz wave activity. Using 10 such orbits, waves were observed near the foreshock boundary for electron plasma frequencies as low as 20 kHz and as high as 54 kHz. We now examine these same 10 orbits to determine how the wave intensity varies with distance along the electron foreshock boundary.

An example from one of the orbits shows a sequence of 30 kHz wave observations from PVO orbit 519 and is illustrated in Figure 2. The OEFD data resolution is .25 seconds and the measurements are taken just upstream of the bow shock crossing at 09:36. Besides distance, additional parameters of depth and θ_{bn} (angle between the intersecting field line and the shock normal at the point of intersection) as well as the magnetic field measurements are included for completeness. We see that the onset of wave activity coincides precisely with connection to the shock, evidenced by the depth parameter changing sign from negative to positive. Though the correlation between wave intensity and depth is clearly evident, it is more difficult to see the correlation between wave intensity and distance from this figure.

In order to show more clearly the correlation between wave intensity and distance, we plot these two parameters (traces 1 and 3 in Figure 2) as a scatter plot in Figure 3. We see a peak in wave intensity around 4 R_V with a subsequent decrease in intensity for greater distances. However, caution must be exercised in that both distance and depth are coupled through the geometry used (i.e. for a particular depth parameter, there is only a finite range of distance parameters available from fluctuations in the IMF). Much of the change in intensity from the peak value seen in Figure 3 is due to increasing depth not distance. To de-couple the two parameters and determine how intensity changes with distance we only use the peak value observed at the foreshock boundary.

Scatter plots such as that in Figure 3 were generated for each of the 40 discrete wave groups observed in the 10 orbits we examined. The distance of the largest median value was recorded together with the peak intensity at that distance. The full data set of all 40 points (0 to 50 R_V in distance) is shown in Figure 4. The regression shows a overall decrease in intensity with distance which is significant at the 90% confidence level. In the bottom portion of this figure we evaluate the region nearer the tangent point (0-15 R_V) which seems to show an increase in intensity with distance and an absolute peak in the range from 3 to 5 R_V. However, the regression is not significant at the 90% level. Reduced data sets, using data associated with an electron plasma frequency within the instrument bandwidth (25-35 kHz), show larger correlation coefficients in the regression, but due to reduction in the number of points no improvement in confidence.

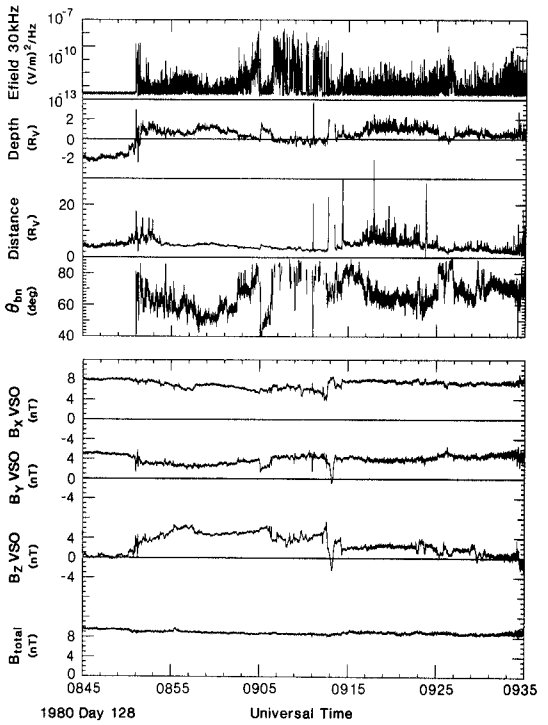

Fig. 2. Sequence of wave observations (OEFD 30 kHz channel) from orbit 519. The onset in activity clearly coincides with magnetic connection to the shock at 08:53 (observed as a change in sign of the depth parameter).

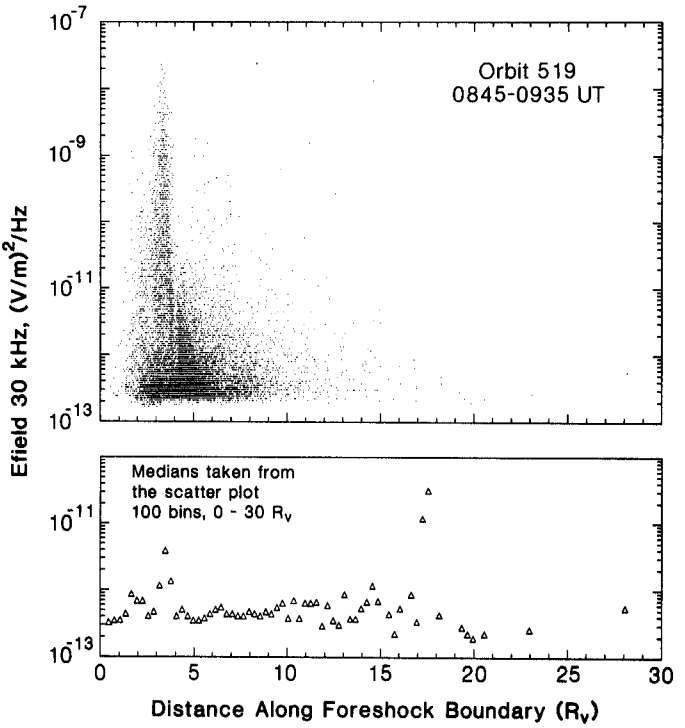

Fig. 3. Scatter plot showing the dependence of wave intensity on distance. The 30 kHz wave data shown in Figure 2 is plotted as a function of distance.

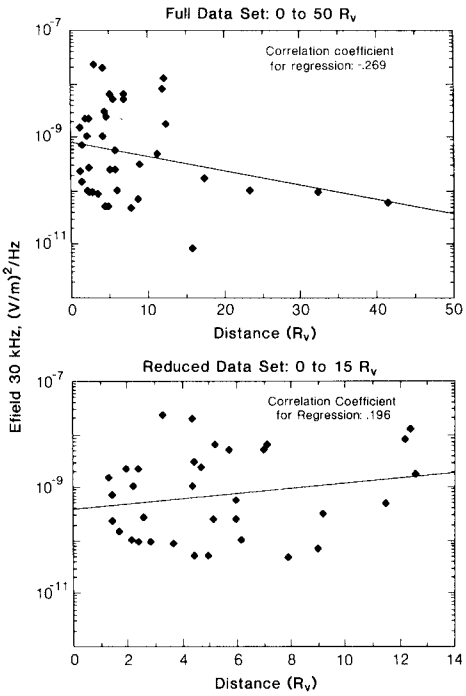

Fig. 4. Peak intensity as a function of distance along the electron foreshock boundary.

CONCLUSIONS

Waves are observed at varying distances along the electron foreshock boundary as measured from the point of tangency. Although not statistically significant at the 90% level, we have found that the peak wave intensity seems to increase with distance to a peak value for the region on the boundary close to the point of tangency (0-15 R_v). The observed decrease in intensity with distance from the peak is significant at a 90% confidence level and is thought to illustrate the general wave behavior along the foreshock boundary. It is possible our observations are linked with the instability process; the instability of the distribution function may increase with distance from the tangent point to saturation at the observed peak, subsequently becoming more stable with greater distance due to scattering of the beam.

ACKNOWLEDGEMENTS

This work was supported by NASA under grants NAG2-485 and NAG2-501.

REFERENCES

1. T-L. Zhang, J.G. Luhmann and C.T. Russell, The solar cycle dependence of the location and shape of the Venus bow shock, *J. Geophys. Res* , 95,14,961 (1990).

2. E.W. Greenstadt, Phenomenology of the Earth's bow shock system. A summary description of experimental results, in: Magnetospheric Particles and Fields, ed. B.M. McCormac, D. Reidel, Hingham, MA, 1976.

3. P.C. Filbert and P.J. Kellogg, Electrostatic noise at the plasma frequency beyond Earth's bow shock, *J. Geophys. Res.*, 84, 1369 (1979).

4. S.A. Fuselier, D.A. Gurnett and R.J. Fitzenreiter, The downshift of electron plasma oscillations in the electron foreshock region, *J. Geophys. Res.*, 90, 3935 (1985).

5. T.G. Onsager and R.H. Holzworth, Measurement of the electron beam mode in Earth's foreshock, *J. Geophys. Res.*, 95, 4175 (1990).

6. G.K. Crawford, R.J. Strangeway and C.T. Russell, Electron plasma oscillations in the Venus Foreshock, *Geophys. Res. Lett* , in press (1990).

7. F.L. Scarf, W.W.L. Taylor and P.F. Virobik, The Pioneer Venus orbiter plasma wave investigation, *IEEE Trans. Geosci. Remote Sens.*, GE-18, 36 (1980).

8. C.T. Russell, R.C. Snare, J.D. Means and R.C. Elphic, Pioneer Venus orbiter fluxgate magnetometer, *IEEE Trans. Geosci. Remote Sens., GE-18*, 32 (1980).

9. C.T. Russell, E. Chou, J.G. Luhmann, P.R. Gazis, L.H. Brace and W.R. Hoegy, Solar and interplanetary control of the location of the Venus bow shock, *J. Geophys. Res.*, 93, 5461 (1988).